

## Catalytic technology assisted with ionization/ozonization phase for the abatement of volatile organic compounds

Antonella Gervasini\*, Vittorio Ragaini

*Dipartimento di Chimica Fisica ed Elettrochimica, Università degli Studi di Milano, Via C. Golgi 19, I-20133 Milano, Italy*

### Abstract

The catalytic combustion process of air-mixtures containing volatile organic compounds (VOCs) associated with an ionization/ozonization reactor (IOCC technique, ionization–ozonization–catalytic-combustion) has been utilized for the abatement of two very toxic industrial VOCs: acrylonitrile (ACN) and vinyl chloride (VCM). The pre-catalytic effects (electric discharge plus the action of ozone), the conventional and IOCC combustion tests were studied. Two different catalysts were used: oxide catalyst, copper–chromite (Cu–Cr), and Pt metal catalyst (0.5 wt.% Pt/ $\gamma$ - $\text{Al}_2\text{O}_3$ ).

The abatement of ACN was markedly influenced by the pre-catalytic effects. Starting from 3 kV, an increasing abatement of ACN was observed with the voltage applied to the ionization reactor at any initial ACN concentration (500–1500 ppm). The ACN catalytic combustion, performed by the IOCC technique, led to 91 and 98% yield of  $\text{CO}_2$  on Cu–Cr and Pt catalysts, respectively, at 260°C. Complete absence of hazardous intermediates, such as hydrogen cyanide, was observed.

The Cu–Cr catalyst, at 300°C, was able to abate 57 and 23% of VCM at 10 000 and 20 000  $\text{h}^{-1}$ , respectively. IOCC combustion led to improved conversion. At 200°C and 3300  $\text{h}^{-1}$ , 98% and only 49% of VCM abatement operating according to IOCC and classical combustion was obtained, respectively. The IOCC combustion runs, performed at different initial VCM concentrations (585 and 1170 ppm), indicated a superior abatement when low VCM concentration was fed, at a given catalyst temperature and contact time. This indicated a marked influence of the pre-catalytic effects on the abatement. © 2000 Elsevier Science B.V. All rights reserved.

**Keywords:** Catalytic combustion; Catalyst; Volatile organic compounds; Acrylonitrile; Vinyl chloride

### 1. Introduction

The harmful effect on human health and on the environment due to different volatile organic compounds (VOCs) vented from many different chemical processes and manufacturing industry imposes their recover or elimination. Total elimination or, at least, abatement below the concentration level fixed by legislation of different countries is expected. The cleaning of gaseous streams containing VOCs in low

concentration (around 1000 ppm) can be achieved by catalytic combustion process that converts the organics into harmless compounds such as water vapor, carbon dioxide, hydrogen chloride, and others, depending on the chemical composition of the organic compounds [1–3]. The catalytic process can be effective at a temperature interval of 300–500°C, which is lower than the temperatures required by the thermal combustion process (1000–1200°C).

The conventional catalytic incineration treatment is a well-established technology for ordinary volatile hydrocarbons. Unfortunately, such an approach can be inappropriate for treating on a large scale industrial wastes containing chlorinated VOCs [4] and organic

\* Corresponding author. Tel.: +39-02-26603-293;  
fax: +39-02-70638-129.  
E-mail address: antonella.gervasini@unimi.it (A. Gervasini)

compounds containing other atoms such as Br- and N-VOCs due to some amount of incomplete combustion products (PICs) and hazardous intermediates formed.

To improve and increase the combustion of air-VOCs, an innovative technology has been proposed, in which a reactor of ionization is coupled with a catalytic reactor: IOCC technique (ionization–ozonization–catalytic-combustion) [5–7]. First, the VOC–air mixture passes through the ionization reactor in which the electric discharge occurs and then it enters into the catalytic reactor in which the oxidation reaction occurs. Moreover, the electric discharge produces ozone by ionization of air (corona effect) [8,9]. The combined pre-catalytic effects of ionization plus ozonization start the demolition of the molecular structure of the organic compounds [10–13], then their complete oxidative degradation is accomplished by the oxidizing catalyst. The IOCC technique is particularly suitable for treating low concentrations of VOCs (maximum  $10^3$  ppm), while gas-streams containing higher VOC concentrations can be recovered by different physical operations (i.e., condensation or absorption).

There are several types of catalysts useful for complete combustion of VOCs. Four big families can be recognized [2,14]: (1) Pt/Pd supported on ceramics; (2)  $V_2O_5/WO_3$  supported on  $TiO_2$ ; (3) Cr-based oxides/zeolites; (4) others. Platinum group metals are well-known active oxidizing catalysts, possessing high resistance to halogen poisoning [4,15–18]. Chromium oxides too are used as catalysts for total oxidation of VOCs. Their effectiveness has been verified by our group for some years (5–7). Corella and coworkers [14] have recently reviewed the effectiveness of catalysts based on chromium oxides by comparing the activity and life of some Cr-based catalysts under “real” flue gas as feedstock.

This work is focused on the abatement of acrylonitrile (ACN) and vinyl chloride (VCM) which are very toxic organic compounds (threshold limit value, TLV, of 20 and 4.55 ppm, respectively [19]) and they are largely used as important intermediates for resins, fibers, elastomers, and polymer production.

ACN, produced by the vapor-phase catalytic ammoxidation of propene, Sohio process, represents the starting material for a very wide range of chemical and polymer products. Acrylic fibers remain as

the largest use of ACN; other significant uses are in resins (acrylonitrile–butadiene–styrene (ABS) and styrene–acrylonitrile (SAN) resins), nitrile elastomers and as intermediate in the production of adiponitrile and acrylamide. ACN, which is highly toxic, has been categorized as a cancer hazard by OSHA [20].

VCM has gained worldwide importance because of its industrial use as the precursor to PVC; it is also used in a wide variety of copolymers. The flame-retardant properties, wide range of plasticized compounds, and the low cost of the polymers from VCM have made it a major industrial chemical. Nearly all the production of VCM is conducted by the balanced process from ethylene and chlorine, with no net consumption or production of HCl. VCM emissions in the balanced process occur from a number of sources, the main ones are the VCM purification system vents and the product loading facility vents. VCM is highly toxic and it is an OSHA-regulated material [21]. The production, manufacture, and abatement of VCM give rise to considerations about the impact of chlorine chemistry on the environment. Hazardous compounds, such as polychlorinated dibenzodioxins, dibenzofurans, and biphenyls (PCDD, PCDF, and PCB, respectively) can be formed when treating chlorinated compounds.

We present the results obtained for the abatement of small concentrations of ACN and VCM contained in air streams. The abatement of such organic compounds is particularly hard to manage due to the possible formation of hazardous N- and Cl-byproducts. Conventional catalytic combustion and IOCC reactions have been compared with the use of the copper–chromite (Cu–Cr) and Pt-based catalysts. Particular interest was devoted to the pre-catalytic effects of ionization and ozonization in the IOCC process on the abatement of the two organic compounds.

## 2. Experimental

ACN and VCM were commercial products of guaranteed grade purity (>99%). Table 1 lists their principal physical characteristics.

The experiments were performed in a continuous reaction line operating at atmospheric pressure [22]. The tests of catalytic combustion were performed working with space velocities in the range  $2500\text{--}20\,000\text{ h}^{-1}$ , expressed in terms of GHSV. The reaction line con-

Table 1  
Physical properties of ACN and VCM

Property	ACN	VCM
Boiling point (°C)	77.3	−13.4
Freezing point (°C)	−83.5	−153.8
Liquid density (g cm <sup>−3</sup> )	0.806 <sup>a</sup>	0.969 <sup>b</sup>
Vapor density (air=1)	1.8	> 2
Volatility (78°C, %)	>99	—
Vapor pressure (kPa)	11.5 <sup>a</sup>	164 <sup>c</sup>
Critical temperature (°C)	246	156.6
Critical pressure (MPa)	3.54	5.60
Critical volume (cm <sup>3</sup> g <sup>−1</sup> )	3.80	2.70
Autoignition temperature (°C)	481	472
Flammability limits in air (25°C)		
Lower (vol.%)	3.0	3.6
Upper (vol.%)	17.0	33.0

<sup>a</sup> At 20°C.

<sup>b</sup> At −14.2°C.

<sup>c</sup> At 0°C.

sisted of a dosing pump for liquid VOC injection (0.015–0.14 ml min<sup>−1</sup>), a mixing chamber of organic vapors with air maintained at 110°C to prevent condensation of the organic compounds (VOC–air mixtures in the range 500–2000 ppm, with total flow rate in the interval 6–60 Nl h<sup>−1</sup>), a reactor of ionization maintained at 60°C (HRS Engineering, Italy, working at fixed frequency, 1000 Hz; variable peak voltage, 0–12 kV; the electric discharge, i.e., corona effect, produced ozone from air and ionized the organic molecules fed), a catalytic reactor (70 cm long, 1.5 cm i.d., containing roughly 2–3 g of catalyst of 710–500 µm size) inserted in a tube furnace electrically controlled in the temperature range

200–500°C, and analytical detectors such as TOC (total organic carbon, from NIRA, Italy), GC-MSD (gas-chromatograph with mass selective detector, from Hewlett-Packard: GC-HP 5980 series II with MSD-HP 5971A interfaced with MS Chemstation software), and ozone analyzer (from Ozone Analyzer, Model H1, USA). The analyses were performed both directly on the off-streams from the reactor (maintained at about 60°C before entering in the analytical apparatus), and on the condensed off-streams, cooled in a trap at −15°C for 6–7 h.

A system of valves allowed us to perform experiments with different operating modes, thus conventional catalytic combustion (M.1); IOCC combustion (M.2); only ionization/ozonization (M.3) of the air–VOC mixtures. Details have been reported elsewhere [7,22]. Typical IOCC runs were performed with the ionization reactor working at fixed frequency (1000 Hz) and at peak voltage of 8.5 kV.

Two different catalysts were employed: copper–chromite oxide catalyst dispersed on alumina (Cu–Cr) and Pt metal catalyst dispersed on alumina, 0.5 wt.%. Both were kindly supplied by Engelhard, Italy (Table 2) and they were activated in flowing air at 400°C before use.

Several characterization analyses on the two catalysts were performed. Surface analysis with X-ray photoelectron spectroscopy apparatus (XPS, M-Probe from Surface Science Instruments with a monochromatic Al Kα radiation source operating at 1486.6 eV) allowed the determination of the surface composition. Determination of the total surface area (SA in m<sup>2</sup> g<sup>−1</sup>) and porosity were performed by physical

Table 2  
Main characteristics of the catalysts used

Properties	Catalyst	
	Cu–Cr	Pt
Composition (wt.%)	Ba, 5.4; Cu, 23.2; Cr, 21.9	Pt, 0.5
BET surface area (m <sup>2</sup> /g)	110	180
Total pore volume (cm <sup>3</sup> /g)	0.35	0.78
Average pore radius, $r_p$ (Å)	60	85
Metal dispersion (%)	—	59
Metal surface area (m <sup>2</sup> /g <sub>pt</sub> )	—	163
Surface chemical state of metal ion and relative concentration <sup>a</sup>	Ba(II), 100%; Cr(III), 70%; Cr(VI), 30%; Cu(I), 8%; Cu(II), 92%	Pt(0), after reduction

<sup>a</sup> BE (eV): Cu(I), 932.4; Cu(II), 934.5; Cr(III), 576.5; Cr(VI), 579.3; Ba(II), 780.7.

adsorption of  $N_2$  at  $-196^\circ\text{C}$  with an automatic analyzer (Sorpomatic 1900 from Thermoquest). Determination of metal dispersion ( $D_M$  in %) and of metal surface area (MSA in  $\text{m}^2 \text{g}_M^{-1}$ ) of Pt-based catalyst were performed by chemisorption of  $H_2$  at  $30^\circ\text{C}$  operating with an automatic analyzer (Sorpomatic 1990 from Thermoquest). For analysis, the following procedure was carried out, thus a portion of catalyst ( $\approx 0.1$  g) was pretreated by reduction at  $350^\circ\text{C}$  in a flux of hydrogen ( $30 \text{ cm}^3 \text{ min}^{-1}$ ) for 2 h and an evacuation in high vacuum ( $P \approx 10^{-4}$  Torr) at the same temperature for 16 h, later the sample was cooled down to  $30^\circ\text{C}$ . Two isotherms of  $H_2$  adsorption, in the range 0–50 Torr, were separated by evacuation at  $30^\circ\text{C}$  for 1 h. Adsorbed volumes were calculated by fitting the linear portion of each isotherm with a straight line and extrapolating it to a zero pressure. The first isotherm represented the total adsorbed  $H_2$  and the second represented the reversibly adsorbed  $H_2$ , their difference gave the irreversibly adsorbed volume, thus, chemical adsorbed  $H_2$ . The knowledge of the metal density and of the average surface area occupied by one metal atom at the surface (for Pt,  $\rho = 21.41 \text{ g cm}^{-3}$  and  $\sigma = 8.90 \text{ \AA}^2 \text{ atom}^{-1}$ , respectively [23]) permitted to calculate the metal dispersion and the metal surface area, assuming  $H_2$  dissociation on Pt-surface ( $H:\text{Pt}_s=1$ ).

### 3. Results

#### 3.1. Catalyst characterization

The Cu–Cr and the Pt/ $\gamma\text{-Al}_2\text{O}_3$  (Pt) catalysts have been characterized by their main properties.

The microstructure, in terms of surface area and porosity, was determined by physical isotherms of adsorption and desorption of  $N_2$ . The obtained BET surfaces are shown in Table 2. The Pt catalyst had larger surface than that of Cu–Cr, this is probably due to the very low amount of Pt content on alumina (0.5 wt.%), in comparison with the high alumina coating of the active Cu–Cr oxidic phase (30 wt.% in CuO and in  $\text{Cr}_2\text{O}_3$ ).

The pore volume and pore size distribution were calculated from the desorption branch of the isotherm by applying the model of straight, non-intersecting cylindrical pores with the computation algorithm of

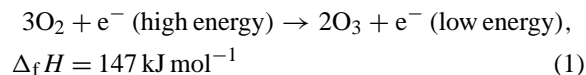
Barrer, Joyner and Halenda (BJH) [24]. The two catalysts presented mesopore distribution centered at about 55 and 75  $\text{\AA}$  of pore radius for Cu–Cr and Pt, respectively. The Pt catalyst had a sharper distribution (from 60 to 80  $\text{\AA}$ ) than that of Cu–Cr (from 20 to 90  $\text{\AA}$ ). This behavior could be expected on the basis of the complex morphological and structural formulation of the Cu–Cr catalyst compared with that of Pt/ $\gamma\text{-Al}_2\text{O}_3$ . From the classical Gurvitch rule [25] and assuming cylindrical geometry for the pores, the average pore radius,  $r_p$ , could be calculated. The  $r_p$  values, shown in Table 2, agree well with the results of the pore size distributions discussed above.

A detailed XPS analysis on Cu–Cr catalyst has been presented [6]. It is well known [26] in both industrial and environmental situations that Cr(III) and Cr(VI) can inter-convert. The reduction of Cr(VI) to Cr(III) is generally favored in most situations. Two distinct Cu species at different binding energy (BE) could be revealed at 934.5 and at 932.4 eV on the fresh catalyst. They have been assigned to CuO or  $\text{Cu}(\text{OH})_2$  and to Cu(I) species, respectively. Regarding the presence of Cr, Cr(III), at 576.5 eV, was the dominant species, and at 780.7 eV, Ba(II) was also present on the surface (Table 2). On the used catalyst, a decrease of the Cr(III)/Cr(VI) and of the Cu(I)/Cu(II) ratios with respect to the values of the fresh catalyst (Table 2) could be detected. The precise values of the ratios depended on the type of VOC treated and on the conditions of the catalytic experiment. In any case, this behavior suggests a surface enrichment of Cr(VI) and Cu(II) species of the Cu–Cr catalyst surface that could be ascribed to the oxidizing power of oxygen or ozone. Ozone decomposition could lead to oxygen radicals on the catalyst surface.

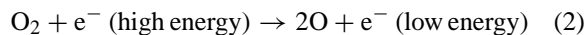
The metal dispersion of the Pt-based catalyst (thus, number of surface Pt atoms with respect to total Pt atoms deposited on the alumina support) was determined following the procedure described in Section 2. Isotherms of  $H_2$  adsorption had a perfect Langmuirian form. The uptake of the irreversibly adsorbed  $H_2$  was used for the calculation of the metal dispersion and the metal surface area (Table 2). Assuming a spherical form for the metal particles, an average diameter of the Pt aggregates of 17  $\text{\AA}$  could be estimated.

### 3.2. Pre-catalytic effects: production of ozone

The ionization of streams of air occurring in the ionization reactor by electric discharge (i.e., corona effect) produced non-negligible amount of ozone by the following reaction [9]:



that can be described by two-step reactions:



Then, ozone can decompose thermally to oxygen



( $E_a = 134 \text{ kJ mol}^{-1}$ , calculated in presence of 22 wt.%  $\text{O}_2$ ).

Ozone is a powerful oxidizing agent, exceeded in its oxidation potential only by fluorine. The strong electrophilic nature of ozone imparts to it the ability to react with a wide variety of organic and organometallic functional groups [10]. Most of the ozone reactions are based on the cleavage of carbon–carbon double bond and on reaction with nucleophilic compounds.

The amount of ozone produced in the ionization reactor increased linearly with the applied voltage in the reactor (Fig. 1). The ozone production increased with lowering the air-flow rate (e.g., at 7 kV,  $\text{O}_3$  concentrations of 758, 1060, and 2515 ppm were detected for air flux at 30, 20, and  $10 \text{ l h}^{-1}$ , respectively). Moreover, the threshold of voltage at which ozone could be detected increased with the air-flow rate. In Fig. 1, two points, corresponding to ozone concentrations determined by iodometric titration [7], have been added to assess the reliability of the measurements made.

During the IOCC runs, the ionization reactor was fed with VOC–air mixture and operated at fixed voltage, therefore, the amount of  $\text{O}_3$  formed was expected to decrease compared to that produced in the sole presence of air, as the electron impact is active both towards the oxygen and the organic molecule.

The oxidizing power of ozone toward VOCs could be expressed in the gas-phase and probably on the catalyst surface too [7]. However, the ozone decay at temperatures higher than  $200^\circ\text{C}$  is very fast. Only at

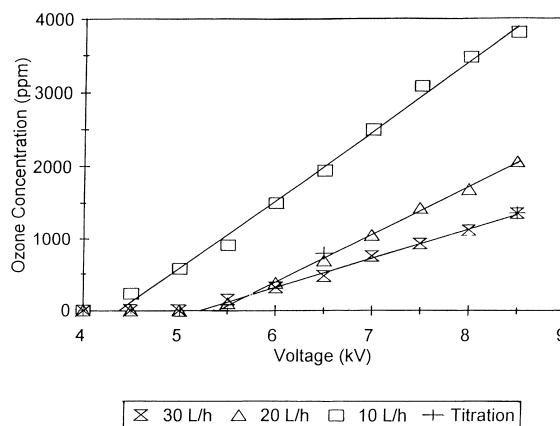


Fig. 1. Ozone production from air by electron discharge as a function of voltage applied in the ionization reactor maintained at  $60^\circ\text{C}$  for different air-flow rates.

low temperatures, ozone could reach the catalyst on which it could decompose giving rise to formation of oxygen radicals, active toward the oxidation of the organic compounds. In addition, the presence of solid catalysts assured its complete decomposition at the outlet of the catalytic reactor [27].

### 3.3. ACN abatement

The chemical properties of ACN are closely related to its reactivity. ACN polymerizes readily in the absence of inhibitor when exposed to light and undergoes the reactions typical of nitriles. Moreover, ACN is combustible and ignites readily, producing toxic combustion products such as hydrogen cyanide (HCN) nitrogen oxides, and carbon monoxide.

The effectiveness of catalytic combustion for the purification of flue-gases mixtures containing ACN operating with periodic flow reversals (reverse-process) has been recently proven [28]. In our approach, we compared the catalytic combustion process with that designated IOCC, in which pre-catalytic effects, such as ionization (electron impact) and ozonization, can attack the ACN molecule in the gas-phase facilitating the successive catalyst action [5–7].

First, we controlled the influence of the pre-catalytic effects on ACN, varying the initial ACN concentration (510–1530 ppm) and the flow rate of the ACN–air mixture in the reaction line ( $10\text{--}30 \text{ l h}^{-1}$ , corresponding to residence times in the reactor of ionization

in the range 42–14 s, respectively) for voltages applied in the reactor up to 8.5 kV (M.3 experiments). Fig. 2 presents the results obtained in terms of residue concentration of ACN, evaluated directly from the off-streams of the reactor by GC-MSD, as a function of the voltage applied in the ionization reactor. Starting from 3 kV of voltage, a decrease of ACN concen-

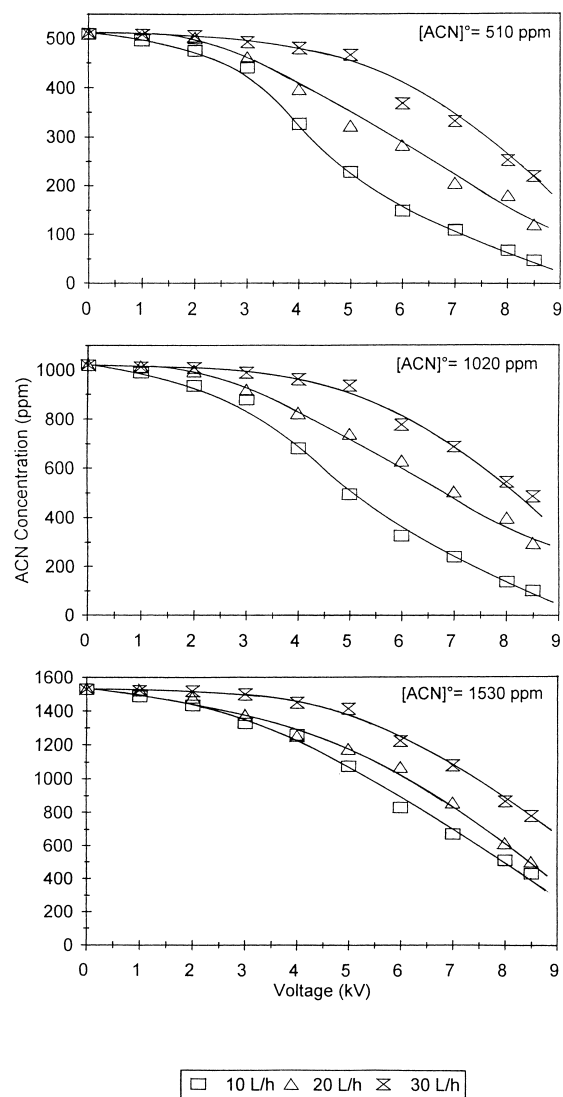


Fig. 2. Influence of the air-flow rate on the ACN residue concentration from the experiments performed according to the method M.3 (ionization and ozonization effects) as a function of voltage applied in the ionization reactor maintained at 60°C for different initial ACN concentrations.

tration in the off-streams was revealed for any initial ACN concentration fed. Considering that the ozone production started at 4.5–5.5 kV, which depends on the air-flow rate (Fig. 1), the initial ACN abatement could be ascribed to the electron impact that shattered the molecule. Increasing the voltage, the ACN residue concentration regularly decreased, reaching values as smaller as the initial concentration fed, operating at 8.5 kV. The sum of the ionization and ozonization effects were now active, as proven by other series of experiments detailed in [7]. A similar trend could be observed at any initial ACN concentration fed, a decrease of the ACN abatement with increasing low rate of ACN–air mixture for a given voltage. For example, at 7 kV and for 510 ppm of ACN initial concentration, values of abatement of 78, 60, and 35% have been obtained for 10, 20, and 30  $\text{L h}^{-1}$ , respectively. Considering that higher flow rates are associated to lower residence times of the ACN–air mixture in the ionization reactor, the observed behavior is due to the influence of the time-factor on the reaction of shattering of the organic molecule by the electron impact. From Fig. 2, the effect of the flow rate of the ACN–air mixture on ACN abatement can be visualized. The curves obtained at different flow rates had similar decreasing trends independent of the ACN concentration. Significant abatements (15–20%) were observed starting from 3, 4, and 6 kV for 10, 20, and 30  $\text{L h}^{-1}$ , respectively. For instance, at 8 kV and 1020 ppm of ACN initial concentration, the abatement was 40, 50, and 80% at 30, 20, and 10  $\text{L h}^{-1}$  as total flow rate, respectively. All the results obtained have been mathematical treated (Statistical Analysis Software, SAS®) to fit the experimental data with calculated curves. As a general trend, the fitting was satisfactory for any set of ACN concentration. The employed equation contained a second law of the voltage and a negative relation with the flow rate.

In successive sets of experiments, catalytic combustions of ACN were performed. The conventional catalytic combustion on Cu–Cr catalyst has been already presented [7], showing the effectiveness of this type of catalyst. In the present work, the Pt-based catalyst was compared with the Cu–Cr one, operating at two temperatures (220 and 260°C) and feeding 1020 ppm of ACN in air at 10 000  $\text{h}^{-1}$  of space velocity (corresponding to 20  $\text{L h}^{-1}$  of the reactant flow). In this case, two different types of analysis were performed, first

a direct evaluation of the conversion of ACN to  $\text{CO}_2$ , from the catalytic reactor off-streams, and secondly a successive analysis of the condensed off-streams, to individuate the by-products formed from incomplete combustion. Fig. 3 shows the results of the combustion of ACN performed by two different modes (conventional combustion, M.1, and IOCC, M.2). The ACN combustion performed by conventional catalytic combustion gave yields to  $\text{CO}_2$  of 20 and 79% at 220°C and 260°C, respectively, on Pt-based catalyst. On Cu–Cr catalyst, the  $\text{CO}_2$  yield was 59 and 83% at 220 and 260°C, respectively. The ACN conversion increased with temperature more on the Pt catalyst than on the Cu–Cr one, as expected, due to the higher activation energy of the noble metal-based catalysts compared with the oxide catalysts [2]. The IOCC runs

gave higher yields to  $\text{CO}_2$  at any temperature and with both catalysts. In particular, on the Pt-based catalyst at lower temperature, very high increase of ACN conversion was obtained, yields to  $\text{CO}_2$  of 76 and 98% were observed at 220 and 260°C, respectively. The ACN conversion was more lightly improved with IOCC runs on the Cu–Cr catalyst (69 and 91% of  $\text{CO}_2$  formed at 220 and 260°C). The electron impact of ionization was responsible for the improvement of the ACN conversion by a gas-phase step of shuttering of the ACN molecule. The very high increase of ACN conversion, observed on Pt-based catalyst at low temperature, could also suggest a positive role of the ozone in the heterogeneous phase. Ozone could give active oxygen radicals on the Pt-surface promoting the ACN conversion.

HCN, was observed among the gaseous off-streams at the two reaction temperatures only on the Cu–Cr catalyst operating by the conventional catalytic combustion, and for instance, at 220°C about 400 ppm of HCN was detected. IOCC runs gave rise to clean abatement of ACN without formation of HCN on both catalysts. Complete absence of other by-products among the gaseous and the condensed off-streams were observed at any temperature on both catalysts. In the previous work [7], it was reported that the IOCC combustion of ACN on Cu–Cr catalyst led to several by-products that deposited on the walls of the ionization reactor. This could be avoided by maintaining the reactor at 60°C (see Section 2), as done in the present investigation.

### 3.4. VCM abatement

VOCs containing chloride atoms (Cl-VOC) can be efficiently abated from gaseous streams by catalytic combustion at mild reaction temperatures, around 500°C, in comparison with 1200°C utilized in the thermal incinerators [2]. Moreover, since the heats of combustion of Cl-VOCs are low compared to those of VOCs, low temperature operation is desired to minimize external energy consumption.

The IOCC technique has been successfully employed for the abatement of several Cl-VOCs present in air streams at low concentrations. Deep and clean combustions can be accomplished at temperatures lower than 500°C with the use of the Cu–Cr catalyst [5–7,14]. Considering that the C–Cl bond has

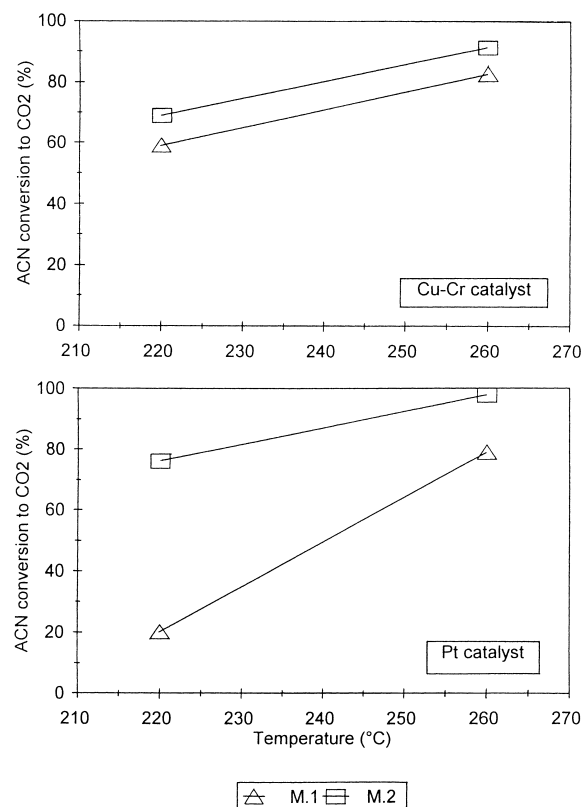


Fig. 3. Conversion of ACN to  $\text{CO}_2$  from combustion runs performed by the conventional catalytic (M.1) and IOCC (M.2) techniques on the two used catalysts (initial ACN concentration, 1020 ppm; space velocity,  $10\,000\text{ h}^{-1}$ ; voltage in the ionization reactor, 8.5 kV).

an average dissociation energy of 338 kJ/mol, lower than those of the C–H and the C–C bonds, 412 and 348 kJ/mol, respectively, the electron impact occurring in the ionization phase can be very effective in shuttering the Cl-VOC molecules.

The VCM combustion was studied comparing the combustion profiles obtained by operating with the techniques of conventional catalytic combustion (M.1) and that of IOCC (M.2). The residue concentration of VCM has been followed as a function of the reaction temperature up to complete combustion. Complete combustion was considered to be reached when the analytical apparatus (TOC) revealed a signal corresponding to 2 ppm or less of total organic carbon in the exhaust gas-stream. Different operative conditions affecting the reaction have been explored: the reaction temperature (from 200 to 450°C) and the VCM initial concentration (from 585 to 1170 ppm). It is known that compounds containing chloride are more difficult to abate than hydrocarbons or oxygenates, then, in order to investigate the performance of the Cu–Cr catalyst towards the abatement of VCM, range of space velocity from 3000 to 20 000 h<sup>-1</sup>, expressed in terms of GHSV, has been studied.

The Cu–Cr catalyst was active towards the combustion of VCM. Fig. 4 shows the results of the VCM abatement as a function of the contact time, expressed

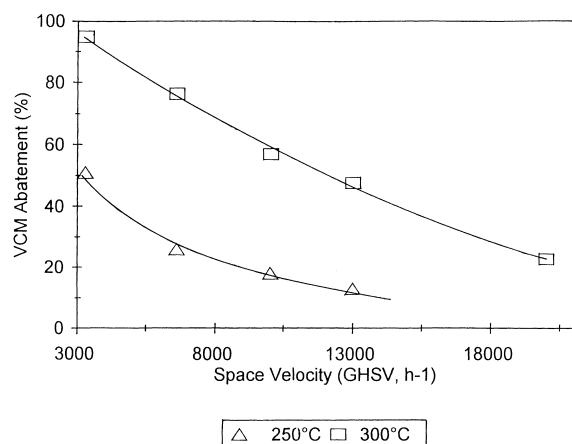


Fig. 4. Abatement of VCM by conventional catalytic combustion on the Cu–Cr catalyst as a function of space velocity, GHSV, at two reaction temperatures. The runs were performed at fixed initial VCM concentration, 585 ppm, and mass of catalyst, 3 g, and varying the VCM–air flow rate from 10 to 60 l h<sup>-1</sup>.

in terms of space velocity (GHSV), at 250 and 300°C. Decreasing curves were obtained, as expected, at the two temperatures. At 300°C and 3300 h<sup>-1</sup> of space velocity, almost complete abatement of VCM could be obtained. Activation energy of 93 kJ/mol could be calculated, assuming a first order rate equation in VCM concentration.

The IOCC technique led to improved VCM combustion compared with the conventional catalytic technique. For example, operating with initial VCM concentration of 585 ppm and 3300 h<sup>-1</sup> of space velocity, VCM was abated at an amount of 98% by the IOCC technique, while only an amount of 49% by the conventional catalytic combustion at 200°C. At higher temperatures, the difference between the combustion profiles obtained with the two catalytic techniques diminished due to the predominance of the catalyst action on the pre-catalytic effects of ionization and ozonization.

The IOCC runs performed at different VCM–air flow rates and fixed initial VCM concentration (1170 ppm) and voltage showed an improved abatement with decreasing the VCM–air flow rate. At 300°C, abatements of 88.5, 95.8, and 99.3% were obtained at 20, 10, and 5 l h<sup>-1</sup>, respectively. This behavior could be expected because low VCM–air flow rates caused an increase of the contact time on the Cu–Cr catalyst and of the residence time of the VCM–air mixture into the reactor of ionization. Then, the catalyst had more time to operate the catalytic action as well as the electron impact that had more time to shutter the organic molecule. To assess this point, different IOCC runs were performed at fixed VCM–air flow rate (10 l h<sup>-1</sup>), i.e., space velocity of 5000 h<sup>-1</sup>, and varying the initial VCM concentration (585 and 1170 ppm). Making comparisons in the range of low temperatures, where the catalyst action is not yet very important, better abatements could be observed when low-concentration of VCM was fed (Fig. 5). This behavior revealed a decisive role not only of the electron impact but also of the ozone in preparing “activated” molecules suitable for the attack of the catalyst. The higher the O<sub>3</sub>/VCM ratio, the larger is the number of organic molecules activated by ozone in the gas-phase. An O<sub>3</sub>/VCM molecular ratio of about 6 and 3 could be calculated feeding 585 and 1170 ppm of VCM, respectively, with a voltage of



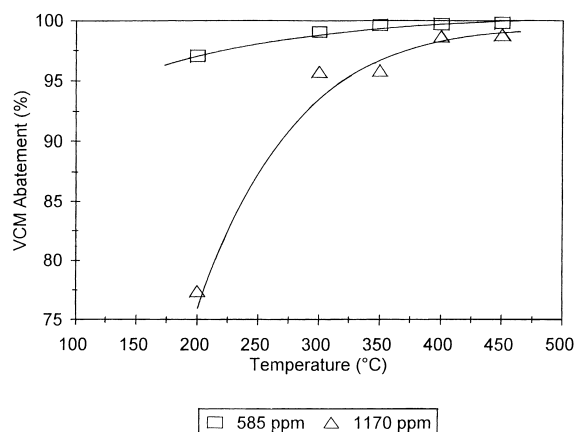


Fig. 5. Abatement of VCM by IOCC technique as a function of temperature for different initial VCM concentrations (space velocity,  $5000\text{ h}^{-1}$ , voltage in the ionization reactor,  $8.5\text{ kV}$ ).

$8.5\text{ kV}$  in the ionization reactor and  $101\text{ h}^{-1}$  of flow rate.

#### 4. Discussion

The potential advantage of ionization/ozonization prior to catalytic abatement holds on the possibility to treat low-temperatures flue-gases. Processes such as solid–liquid and liquid–liquid extraction, liquid and solid dissolution or dilution, degreasing, refilling of fuel tanks are examples of some industrial unit operations in which VOCs can be released in the atmosphere at low-temperatures and low-concentrations.

For industrial application of IOCC technique, problems of energetic costs of the discharge in the ionization reactor have to be taken into account. It can be considered that for this step the energy consumption,  $E$  ( $\text{kW m}^{-3}$ ), depends on the applied voltage,  $V$  ( $\text{kV}$ ), the applied current,  $A$  ( $\text{mA}$ ) for a time  $t$  ( $\text{h}$ ), and the flow of polluted air in the ionization reactor,  $F$  ( $\text{m}^3/\text{h}^{-1}$ ). The following equation results:

$$E = (VA t (F t)^{-1}) \times 10^{-3} \quad \text{or} \quad E = (V A F^{-1}) \times 10^{-3} \quad (5)$$

Alternatively, Eq. (5) can be written considering the volume of the polluted air that corresponded to the volume of the ionization reactor ( $V_R, \text{m}^3$ ), and as time

that corresponded to the residence time of the polluted air into the ionization reactor ( $\tau$ ):

$$\tau = V_R F^{-1} = 1(SV)^{-1}, \quad (6)$$

in which  $SV$  is the space velocity in  $\text{h}^{-1}$ . Therefore, it derives

$$E = [sVA(V_R F^{-1})V_R^{-1}] \times 10^{-3} \quad \text{or} \quad E = [VA(SV V_R)^{-1}] \times 10^{-3} \quad (7)$$

Suitable industrial values of the parameters in Eqs. (5) or (7) are:  $V = 9\text{ kV}$ ;  $A = 100\text{ mA}$ ;  $F = 3000\text{ m}^3/\text{h}^{-1}$ ;  $SV = 10\,000\text{ h}^{-1}$ ;  $V_R = 1\text{ m}^3$ . From these values an energy consumption,  $E$ , of  $9 \times 10^{-5}\text{ kWh m}^{-3}$  is derived. From such value, it can be calculated that the energy required for treating  $10^6\text{ m}^3$  of polluted air is  $90\text{ kWh}$ . The energy consumed in the first-step of the IOCC technique is lower than that required by conventional pre-heating catalytic reactors.

Another problem on the use of ionization reactors in industrial processes is concerning the safety issue. However, it can be considered that there is no danger of explosion events in the ionization reactor provoked by sparks. The corona effect does not lead to any spark. It is necessary to consider that the usual concentration of VOCs for the abatement by catalytic combustion is in the range of ppm (maximum  $10^3$ – $10^4$  ppm). Moreover, the above-mentioned concentrations are well below the usual lowest explosion limits (LELs) for large number of VOCs [19].

#### 5. Conclusion

The IOCC technology can be successfully used for the purification of streams of air containing low concentration of ACN and VCM. The VOC–air flow rate feeding the reactor of ionization/ozonization and the catalytic reactor deeply influenced by the extent of the abatement. This behavior was principally due to the strong influence of the pre-catalytic effects, i.e., the electron impact, causing ionization of the organic compounds, and the oxidizing action of ozone. Comparing the conventional catalytic combustion with that realized with the IOCC technique for the abatement of ACN and VCM, cleaner off-streams from the reactor could be obtained by using the IOCC process. This aspect should be taken into account for the development

of new environmentally clean and safe technologies for the purification of gaseous streams from industries.

It is noteworthy to observe that the ionization/ozonization procedure is operative in a few seconds and therefore could be proposed as an emergencies intervention.

### Acknowledgements

This work was assisted by CNR grant (Progetto Strategico — Gruppo Nazionale per la Difesa dai Rischi Chimico Industriali ed Ecologici). Authors are very grateful to Dr. De Ruvo for making the experiments and to Ing. Bardelli (HRS Engineering, Italy) for the assistance of equipments.

### References

- [1] R. Prasad, L.A. Kennedy, A.E. Ruckenstein, *Catal. Rev.-Sci. Eng.* 26 (1984) 1.
- [2] J.J. Spivey, *Ind. Eng. Chem. Res.* 26 (1987) 2165.
- [3] I.M. Freidel, A.C. Frost, K.J. Herbert, F.J. Meyer, J.C. Summers, *Catal. Today* 17 (1993) 367.
- [4] J.C. Lou, S.S. Lee, *Appl. Catal. B* 12 (1997) 111.
- [5] V. Ragaini, C.L. Bianchi, G. Forcella, A. Gervasini, in: L. Bonati, et al. (Eds.), *Trends in Ecological Physical Chemistry*, Elsevier, Amsterdam, 1993, p. 275.
- [6] A. Gervasini, C.L. Bianchi, V. Ragaini, *ACS Symp. Ser.* 552 (1994) 353.
- [7] A. Gervasini, G.C. Vezzoli, V. Ragaini, *Catal. Today* 29 (1996) 449.
- [8] M. Kirschner, in: *Ullmann's Encyclopedia of Industrial Chemistry*, Vol. A18, 5th Edition, VCH, Weinheim, 1991, p. 349.
- [9] C. Nebel, in: Kirk-Othmer (Ed.), *Encyclopedia of Chemical Technology*, Vol. 16, 3rd Edition, Wiley, New York, 1981, p. 683.
- [10] S.D. Razumovskii, G.E. Zaikov, *Ozone and its Reactions with Organic Compounds*, *Studies in Organic Chemistry*, Vol. 15, Elsevier, Amsterdam, 1984.
- [11] C.M. Nunez, G.H. Ramsey, W.H. Ponder, J.H. Abbott, L.E. Hamel, P.H. Kariher, *Air Waste* 43 (1993) 242.
- [12] E.C. Tuazon, J. Arey, R. Atkinson, S.M. Aschmann, *Environ. Sci. Technol.* 27 (1993) 1832.
- [13] A. Czernichowski, A. Ranaivosoloarimanana, *CHEMTECH* (1996) 45.
- [14] A.M. Padilla, J. Corella, J.M. Toledo, *Appl. Catal. B* 22 (1999) 107.
- [15] J. Hermia, S. Vigneron, *Catal. Today* 17 (1993) 349.
- [16] H. Müller, K. Deller, B. Despeyroux, E. Peldszus, *Catal. Today* 17 (1993) 383.
- [17] J.E. Sawyer, M.A. Abraham, *Ind. Eng. Chem. Res.* 33 (1994) 2084.
- [18] H. Windawi, Z.C. Zhang, *Catal. Today* 30 (1996) 99.
- [19] N.I. Sax, *Dangerous Properties of Industrial Materials*, 6th Edition, Van Nostrand, New York, 1984.
- [20] L.T. Groet, in: Kirk-Othmer (Ed.), *Encyclopedia of Chemical Technology*, Vol. 1, 3rd Edition, Wiley, New York, 1978, p. 414.
- [21] J.A. Cowfer, A.J. Magistro, in: Kirk-Othmer (Ed.), *Encyclopedia of Chemical Technology*, Vol. 23, 3rd Edition, Wiley, New York, 1983, p. 865.
- [22] V. Ragaini, P. Carniti, A. Gervasini, A. Bienati, E. Benfenati, G.C. Vezzoli, in: B. Rindone, P. Beltrame, et al. (Eds.), *Le Emissioni Industriali in Atmosfera*, Fondazione Lombardia per l'Ambiente, Milano, 1998, p. 109.
- [23] R. Giannantonio, V. Ragaini, P. Magni, *J. Catal.* 146 (1994) 103.
- [24] G. Leofanti, M. Padovan, G. Tozzola, B. Venturelli, *Catal. Today* 41 (1998) 207.
- [25] S. Lowell, J.E. Shields, in: B. Scarlett (Ed.), *Powder Surface Area and Porosity*, *Powder Technology Series*, Vol. 8, London, 1984.
- [26] D.E. Kimbrough, Y. Cohen, A.M. Winer, L. Creelman, C. Mabuni, *Crit. Rev. Environ. Sci. Technol.* 29 (1999) 1.
- [27] B. Dhandapani, S.T. Oyama, *Appl. Catal. B* 11 (1997) 129.
- [28] G.V. Vanin, A.S. Noskov, G.Ya. Popova, T.V. Andrushkevich, Yu.Sh. Matros, *Catal. Today* 17 (1993) 251.